Behavioral/Cognitive

Cingulo-Opercular Subnetworks Motivate Frontoparietal Subnetworks during Distinct Cognitive Control Demands

Jessica L. Wood and Derek Evan Nee

Department of Psychology, Florida State University, Tallahassee, Florida 32306-4301

Cognitive control is the ability to flexibly adapt behavior in a goal-directed manner when habit will not suffice. Control can be separated into distinct forms based on the timescale (present–future) and/or medium (external–internal) over which it operates. Both the frontoparietal network (FPN) and cingulo-opercular network (CON) are engaged during control, but their respective functions and interactions remain unclear. Here, we examined activations in the FPN and CON with fMRI in humans (male and female) during a task that manipulated control across timescales/mediums. The findings show that the CON can be distinguished into the following two separable subnetworks mirroring the FPN: a rostral/ventral subnetwork sensitive to future-oriented control involving internal representations, and a caudal/dorsal subnetwork sensitive to present-oriented control involving external representations. Relative to the FPN, activation in the CON was particularly pronounced during transitions into and out of particular control demands. Moreover, the relationship of each CON subnetwork to behavior was mediated by a respective FPN subnetwork. Such data are consistent with the idea that the CON motivates the FPN, which, in turn, drives behavior. Within the CON, the dorsomedial prefrontal cortex (dmPFC) mediated the relationship between the anterior insula and FPN, suggesting that the dmPFC acts as the crux that links the CON to the FPN. Collectively, these data indicate that parallel CON–FPN subnetworks mediate controlled behaviors at distinct timescales/mediums.

Key words: cognitive control; executive function; fMRI; motivation; network interactions; subnetwork

> **Significance Statement**
>
> The cingulo-opercular network (CON) and frontoparietal network (FPN) are engaged in diverse, demanding tasks. A functional model describing how areas within these networks can be distinguished, and also interact, would facilitate understanding of how the brain adapts to demanding situations. During a comprehensive control task, fMRI data revealed that the FPN and CON can be fractionated into subnetworks based on control demands that are either externally oriented for use in the present, or control demands that operate internally to guide future behavior. Moreover, we found evidence for a chain of relationships from the CON to FPN to behavior consistent with the idea that the CON drives the FPN to adapt behavior.

Introduction

Complex demands require juggling current tasks and future plans for the flexible achievement of goals. Cognitive control is used to override automated behaviors, allowing ongoing cognition to be oriented and used in a goal-directed manner. Cognitive control

recruits a broad constellation of cortical areas referred to as the multiple demand system (MDS; Duncan, 2010). While MDS regions show engagement in diverse tasks, connectivity mapping indicates that the MDS is composed of at least two networks: the frontoparietal network (FPN) and the cingulo-opercular network (CON; Dosenbach et al., 2007; Seeley et al., 2007; Yeo et al., 2011). Moreover, there is evidence that the FPN itself is composed of subnetworks (Braga and Buckner, 2017; Dixon et al., 2018; Murphy et al., 2020; Nee, 2021). Some work has also suggested that a more ventrally defined salience network can be distinguished from a dorsally defined CON (Power et al., 2011; Gordon et al., 2016; Gratton et al., 2018). Yet, connectivity alone does not tell us either the function of these subnetworks or how they interact to perform demanding behaviors.

Recent work has begun to characterize the functional roles of subnetworks within the FPN (Dixon et al., 2018; Murphy et al., 2020; Nee, 2021). These works converge on the idea that somatomotor proximal areas are involved in control that is present

oriented and concerned with the external environment, while somatomotor distal areas are involved in control that is future oriented and concerned with internal representations (Nee, 2021). Hence, control processing in the FPN varies along the timescale (present–future) and/or medium (external–internal). Currently, an analogous functional characterization of the CON remains unclear.

One barrier toward understanding the CON is that prior theories have presented conflicting accounts. On the one hand, the CON has been hypothesized to play a sustained role. For example, the CON has been proposed to sustain stable set control (Dosenbach et al., 2006, 2007) and to maintain tonic alertness (Sadaghiani and D'Esposito, 2015). These sustained processes are in contrast to phasic "rapid adaptive control" initiation by the FPN (Dosenbach et al., 2008). Other accounts propose that CON areas perform more transient processes. For example, one model proposes that cingulo-opercular areas initiate dynamic switching between the internally related default mode network (DMN) and the externally driven FPN (Menon and Uddin, 2010). Furthermore, a transient role in cognition is often attributed to the anterior cingulate cortex (ACC) of the CON in signaling conflict (Botvinick et al., 2001), prediction errors (Alexander and Brown, 2011), and the expected value of control (Shenhav et al., 2013). In these models, transient ACC signals are thought to drive adjustments in the sustained control processes instantiated by the FPN. Hence, different models conflict with their attribution of transient versus sustained roles to the CON versus FPN.

The conflicting roles of the CON and FPN may arise from a failure to properly appreciate distinct functional properties of subnetworks therein. Data reviewed above suggest that the FPN has a temporal axis such that somatomotor proximal areas act in the immediate term while somatomotor distal areas act over longer timescales (see also Fuster, 2001; Koechlin, 2003; Koechlin and Summerfield, 2007). This suggests that whether the FPN is regarded as transient versus sustained may arise from examining somatomotor proximal versus somatomotor distal areas, respectively. If a similar temporal gradient also exists in the CON, this could resolve conflicting roles that have been ascribed to the CON.

Here, we examined the functional roles of areas within the CON and FPN, and how these areas interact to support cognitive control. We reanalyzed human fMRI data during a task that previously provided functional characterizations of FPN subnetworks (Nee and D'Esposito, 2016, 2017; Nee, 2021). First, we examined whether the CON can be fractionated into functional subnetworks in a manner that parallels the FPN. Next, we examined whether distinct transient versus sustained roles could be attributed at the network and/or subnetwork level. Finally, we leveraged the relationship of each subnetwork with behavior at distinct timescales to test interactions between the CON and FPN.

Materials and Methods
Experimental design
Participants. Two separate samples of young, healthy participants were previously collected (described in detail in Nee and D'Esposito, 2016, 2017). Sample 1 consisted of 24 participants (13 females; mean age, 19.9 years; age range, 18–28 years). Sample 2 included 25 participants (16 females; mean age, 20.6 years; age range, 18–27 years). All participants were right-handed English speakers with no reported history of neurologic or psychiatric conditions. Informed consent was obtained in accordance with the University of California, Berkeley, Committee for Protection of Human Subjects.

Task. The comprehensive control task (Fig. 1) was designed and described in full in the study by Nee and D'Esposito (2016), and adapted

from previous work (Koechlin et al., 1999; Charron and Koechlin, 2010). The task was designed to manipulate the following three proposed control demands: temporal control (TC), or future oriented planning; contextual control (CC), or adapting behavior based on rules; and sensory-motor control (SM), or linking stimulus to action. These control demands vary as a function of timescale as temporal control is future oriented, sensory-motor control is present oriented, and contextual control is in-between. These demands also vary over medium as temporal control involves sustaining and referencing internal representations, sensory-motor control involves processing externally oriented representations of both perception and action, and contextual control involves the joint consideration of these mediums (Nee, 2021). Each condition was additionally completed across the following two stimulus domains: verbal and spatial, such that domain specificity versus domain generality can further distinguish the extent to which control processes are sensitive to specific stimulus demands (i.e., more externally oriented); or generalize across stimulus demands.

The primary task involved sequence-back decisions in which participants used a learned sequence to identify whether the current stimulus followed the previous stimulus within the sequence. For example, on verbal conditions the learned sequence was the order of letters in the word "TABLET" (i.e., "T" is the beginning, "A" follows "T," and so on). In the spatial conditions, the sequence was the order of locations of the points on a five-pointed star (i.e., the top point was the start of the sequence, followed by the bottom-right point, followed by the top-left point, and so on). As both stimulus domains were present on each trial (i.e., a letter was shown at a point in the star), the relevant stimulus domain was cued by the color of the shape surrounding the letter (e.g., blue square for verbal and yellow square for spatial), which remained constant for the duration of a block.

During the first trial of a 7–13 trial block, participants determined whether the stimulus was the first item in the sequence (i.e., "T" or top; sequence-start). Subsequent stimuli were compared with the preceding stimulus to determine whether they followed in the order of the sequence (sequence-back). All trials required a "yes" or "no" response using a left or right button press with response mappings counterbalanced between participants.

Following the initial sequence-start trial, each block continued with one to four trials of sequence-back. In the baseline condition, sequence-back continued throughout the remainder of the block, engaging sensory-motor control to select the appropriate action for the presented stimulus. These trials were cued by square-shaped frames. In other conditions, a shape change cued the participant to begin three to five subtask trials that altered the control demands. In the restart condition, a shape change (e.g., from square to circle) cued the participant to restart the sequence (i.e., determine whether the stimulus was the beginning of the sequence, regardless of where they were previously). Participants resumed sequence-back thereafter until the shape changed again (e.g., from circle to square), at which point they would once again restart the sequence. Thus, the restart condition required participants to switch among tasks (sequence-back and sequence-start) adding contextual control to select the appropriate task set. In the delay condition, a different shape change (e.g., from square to diamond) signaled the participant to remember their current place in the sequence for a future trial. Upon return to the original shape (e.g., from diamond to square), participants determined whether the current stimulus followed the previous stimulus of the same shape. For trials in-between (e.g., diamond-framed trials), participants acknowledged stimuli with a "no" keypress, but no further processing was required. Hence, the delay condition removed demands on sensory-motor control, while adding demands on temporal control to prepare for the future. Finally, in the dual condition, the restart and delay rules were combined. Here, shape changes (e.g., square to cross) cued participants to remember their current place in the sequence for a future trial, while also restarting the sequence (e.g., perform sequence-start on the first cross-framed trial, and sequence-back on subsequent cross-framed trials). Upon return to the original shape (e.g., from cross to square), the participant determined whether the stimulus followed the previous stimulus of the same shape. Hence, the dual condition added both contextual control to select among task sets, and temporal control
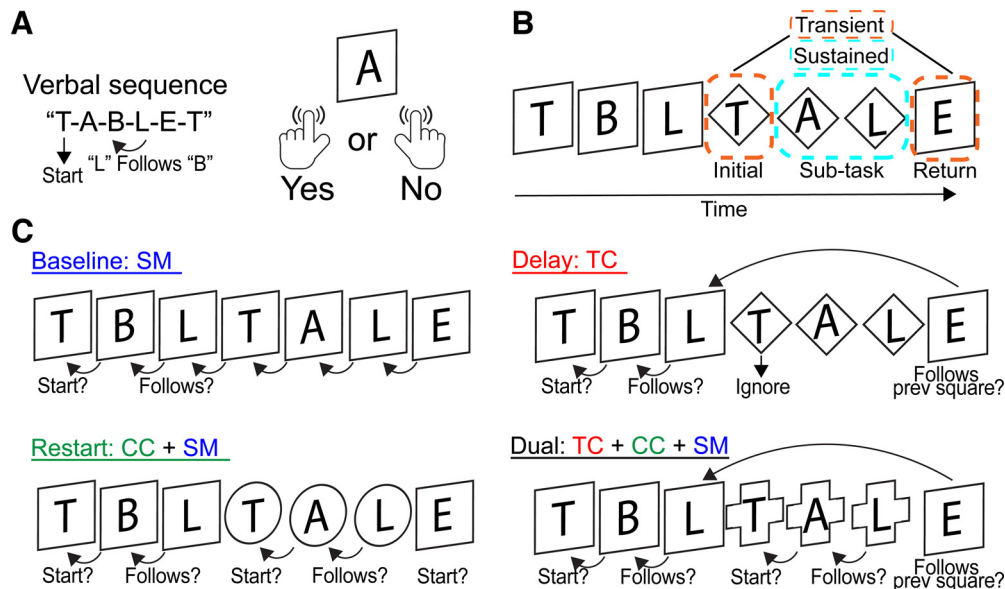
Figure 1. Comprehensive control task. **A**, Participants learned a sequence—the order of letters in the word TABLET—to determine whether the letter presented on the screen followed the previous letter in the sequence (sequence-back) by making a yes/no button response. Actual letters were presented in one of five spatial locations with the spatial locations forming an analogous spatial sequence. For simplicity, only the verbal stimulus domain sequence is presented with letters depicted centrally for ease of exposition. **B**, Schematic of the task broken down into phases used for analysis. The initial and return trials were combined to form the transient phase, and the subtask trials in-between (which coincided with different rules in each condition) made up the sustained phase. **C**, In all conditions, blocks began with a determination of whether the stimulus is the start of the sequence (sequence-start), followed by trials of the sequence-back task, which required sensory-motor control (SM) to select the appropriate action associated with the stimulus (square shape); continuation of the sequence-back task made up the baseline condition. In the restart condition, a shape change (circle) cued the participant to restart the sequence, adding contextual control (CC) to select the appropriate task (sequence-start or sequence-back). In the delay condition, the participant needed to plan for a future trial while pressing "no" to each stimulus (ignore; diamond), using temporal control (TC) to sustain an internal representation for the future. The dual condition combined both restart and delay rules requiring sensory-motor, contextual, and temporal control. For further description, see Materials and Methods and the study by Nee and D'Esposito (2016, 2017).

to prepare for the future. All blocks concluded with one to two trials of sequence-back cued by square frames.

To summarize, baseline blocks required a steady state of sensory-motor control. Other blocks began with an initial phase of sensory-motor control, followed by a subtask phase that altered control demands, and concluded with a final phase of sensory-motor control.

The subtask phase of each block, which is of main interest, was designed to factorially vary stimulus domain (verbal, spatial), temporal control (high = delay and dual, low = baseline and restart), and contextual control (high = restart and dual, low = baseline and delay), resulting in a $2 \times 2 \times 2$ design. In addition, sensory-motor control was also varied across conditions (high = baseline, restart, and dual, low = delay). This design allowed for the identification of control demands through orthogonal contrasts of the control demands while marginalizing over stimulus domain: main effect of temporal control = (dual + delay) – (restart + baseline); main effect of contextual control = (dual + restart) – (delay + baseline); and sensory-motor control = (dual + baseline) – (restart + delay). The sensory-motor control contrast is effectively the interaction term of the temporal control and contextual control factors. Finally, stimulus domain could be examined through the main effect of stimulus domain while marginalizing over control demands (e.g., all verbal – all spatial). In the present report, we focus primarily on the contrasts of temporal control and contextual control as defined above.

Color–stimulus domain and shape–task mappings were counterbalanced between participants. Participants completed 12 runs (sample 1) or 6 runs (sample 2) of 16 blocks each, totaling 1920 (sample 1) or 864 (sample 2) trials.

Present analyses focus on the following three phases for each block: (1) the first shape-change trial [i.e., from square to alternate shape, which initiated a new control demand (initial)]; (2) subsequent subtask trials, which sustained the control demands (subtask); and (3) the second shape-change trial [i.e., from alternate shape to square, which concluded the control demand (return)]. Since baseline blocks included no shape change, trials were chosen in the middle of the baseline block to match the other blocks in cadence and length. For analysis, the initial and

return trials were averaged together to define the transient phase, whereas the subtask trials defined the sustained phase (Fig. 1B).

fMRI procedure. Each sample was trained on the behavioral task outside of the scanner within a week before the fMRI session to ensure understanding and apt practice of the task. Sample 1 completed two scanning sessions, and sample 2 completed a single session. All scans were collected on a Siemens TIM/Trio 3T MRI equipped with a 32-channel head coil located in the Henry H. Wheeler Jr. Brain Imaging Center at the University of California, Berkeley. Stimuli were projected to a coil-attached mirror using an MRI-compatible projector (Avotec; https://avotecinc.com). Experimental tasks were created using E-Prime software version 2.0 (Psychology Software Tools; https://pstnet.com/). Eye position was monitored using an Avotec system (model RE-5700) and Viewpoint software (http://www.arringtonresearch.com/). Response data were collected on an MR-compatible button box (Current Designs; https://curdes.com).

T2*-weighted fMRI was performed using gradient echoplanar imaging with $3.4375\ mm^2$ in-plane resolution and 35 descending slices of 3.75 mm thickness (TR = 2000 ms; echo time = 25 ms; flip angle = 70; field of view = $220\ mm^2$). The first three images of each run were automatically discarded to allow for image stabilization. Field maps were collected to correct for magnetic distortion. High-resolution T1-weighted MPRAGE images were collected for anatomic localization and spatial normalization ($240 \times 256 \times 160$ matrix of 1 mm^3 isotropic voxels; TR = 2300 ms; echo time = 2.98 ms; flip angle = 9).

fMRI processing. Preprocessing was performed in SPM12, unless otherwise noted. Raw images were converted from DICOM to nifti format, and origins were manually set to the anterior commissure. The AFNI 3dDespike routine was used for spike correction on functional data. Slice-timing corrections and spatial realignment were then performed to correct for differences in timing and spatial position, respectively. Images were corrected for distortion and movement-by-susceptibility artifacts (Andersson et al., 2001). The functional data were coregistered to the T1-weighted image, which was segmented and spatially normalized to the MNI template. The resultant warp was applied to the functional

images, which were also resampled to 2 mm³, and smoothed with a 4 mm full-width at half-maximum isotropic Gaussian kernel. For analysis, a temporal high-pass filter at 128 s was used, as well as temporal autocorrelation corrections using an autoregressive AR (1) model, and scaling such that the run-wide global signal averaged 100.

Statistical analyses

Univariate image analysis. Univariate image analysis was conducted in SPM12. At the first level, the regressors of main interest included the initial trial, subtask phase, and return trial (Fig. 1B), which were separately modeled for each crossing of stimulus domain and block type (i.e., verbal, spatial × baseline, restart, delay, dual). The initial and return trials included transient regressors to model the individual trials, whereas the subtask phase was modeled as an epoch starting after the first subtask trial through the end of the final subtask trial. Transient regressors were included to model left and right button-presses. Additional transient regressors were included for the first trial of each block, separately for each stimulus domain. Additional epoch regressors were included separately for the trials preceding and following subtask phases, again separated by stimulus domain. Finally, errors during any epoch phase were captured by a separate transient regressor. All regressors were convolved with the canonical hemodynamic response function implemented in SPM. All models included 14 motion regressors reflecting linear (6 regressors) and squared (6 regressors) movement parameters, framewise displacement (1 regressor), and squared framewise displacement (1 regressor) to remove motion-related artifacts (Lund et al., 2005; Power et al., 2012; Satterthwaite et al., 2013). Additionally, regressors were separately included for each TR with a framewise displacement exceeding 0.5 to censor the frame.

The model described above was used to define regions of interest (ROIs). However, on adding in transient versus sustained analyses with our CON ROIs, we subsequently noted that error responses during initial and return trials were not modeled separately as they were during epoch phases (note, this was not an issue in our past work using these data, as these data were reprocessed for the present study for training purposes). To ensure that these errors did not unduly influence estimates of transient control, we ran a second model that excluded and separately modeled all initial and return trials that produced an erroneous response. Data from this second model are used for all reported analyses.

The first-level parameter estimates were carried to the group level model in a 2 × 2 × 2 ANOVA with factors of stimulus domain (verbal, spatial), temporal control (high, low), and contextual control (high, low). The task was designed to form the following five orthogonal contrasts of interest based on each control demand and stimulus domain: (1) temporal control (Dual + Delay > Restart + Baseline); (2) contextual control (Restart + Dual > Baseline + Delay); (3) sensory-motor control (Dual + Baseline > Restart + Delay); (4) verbal domain (Verbal > Spatial); and (5) spatial domain (Spatial > Verbal). In other words, control demands are examined through main effects and interactions of the factorial design. As described previously (Nee and D'Esposito, 2016), although sensory-motor control is not factorially manipulated, it can be examined via subtraction logic by the temporal control × contextual control interaction since this contrast balances out demands on temporal control and contextual control on both sides of the contrast, while leaving demands on sensory-motor control on the left side of the contrast. The control demand contrasts were collapsed across stimulus domain (e.g., Dual is a combination of Verbal-Dual and Spatial-Dual conditions), while contrasts within stimulus domain were collapsed across the control conditions (e.g., Verbal is a combination of Verbal-Dual, Verbal-Delay, Verbal-Restart, and Verbal-Baseline). Whole-brain voxelwise activation maps were thresholded at $q < 0.05$ using false discovery rate to correct for multiple comparisons.

ROI analysis. The 6 mm³ spherical ROIs were defined centered on peak activations from the contrasts of interest. As we detailed previously (Nee and D'Esposito, 2016), ROIs in the lateral prefrontal cortex (PFC) were originally defined by noting, in order, peaks in sample 1 in the temporal control contrast, the sensory-motor control contrast, and the

contextual control contrast. Distinct peaks were defined as local maxima in the lateral PFC at least 1.5 cm from another peak. As it was noted that stimulus domain contrasts (i.e., verbal > spatial, and spatial > verbal) produced peaks similar to those observed in the sensory-motor control, but with better spacing away from other lateral PFC peaks, the sensory-motor peaks were replaced by peaks defined by the stimulus domain contrast [note, sensory-motor control-derived peaks were used to initially test for effects of stimulus domain in the study by Nee and D'Esposito (2016) to ensure orthogonality between ROI definition and testing], but stimulus domain-derived peaks were used for subsequent analyses that were not focused on stimulus domain per se]. Peaks in the lateral frontal pole (FPl; MNI coordinates: −44, 48, 4), and middle frontal gyrus (MFG; −38, 28, 44) in or around the posterior middle frontal sulcus (Miller et al., 2021a, b) were identified by the temporal control contrast. Peaks in the ventrolateral PFC (VLPFC; −52, 20, 28) and caudal MFG (cMFG; −34, 10, 60) were identified by the contextual control contrast. Peaks in the inferior frontal junction (IFJ; −38, 6, 26) and superior frontal sulcus (SFS; −22, 0, 54) were identified by the stimulus domain/sensory-motor control contrasts. The resultant ROIs spanned the rostral–caudal and dorsal–ventral axes of the lateral PFC. Subsequently (Nee and D'Esposito, 2017), peaks in the temporal control, contextual control, and stimulus domain contrasts were noted in sample 2 via analogous methods (FPl: −36, 52, 0; MFG: −36, 34, 38; VLPFC: −42, 30, 20; cMFG: −30, 6, 56; IFJ: −42, 10, 24; SFS: −20, 0, 56). Analogous procedures were then used to identify peaks in the posterior parietal cortex (Nee, 2021) producing peaks in the inferior parietal lobule (sample 1: −54, −50, 44; sample 2: −56, −52, 42), mid-intraparietal sulcus (sample 1: −28, −60, 42; sample 2, −26, −56, 44), anterior intraparietal sulcus (sample 1: −34, −40, 46; sample 2: −30, −42, 42), and superior parietal lobule (sample 1: −14, −52, 64; sample 1: −12, −60, 58). Sample 1 contrast maps were used to define ROIs to test sample 2, and vice versa. This procedure ensures independence between data used to define and test ROIs, thereby providing unbiased estimates of activation.

Following the above procedures, CON ROIs were analogously defined within the dorsomedial PFC (dmPFC) and anterior insula (aI) based on visual inspection of cortical anatomy. However, although topographical gradients that paralleled the FPN were observable in the CON (see Fig. 3), these gradients were condensed in space. Hence, the distance criteria we used to separate peaks in the FPN were more difficult to apply to the CON. In particular, we noted some peak activations across contrasts were <1 cm distance apart, which particularly affected distinguishing contextual control from sensory-motor control-related peaks. To avoid redundancy, we compared the peak activations of each contrast across samples to find the most consistent peak (i.e., the coordinate that was most similar between sample 1 and sample 2) and therefore used the contrast that reflected consistency between samples. Practically, this resulted in the use of contextual control contrasts to define ROIs, although sensory-motor control contrasts provided similar CON activations.

SPM12 scales transient and epoch regressors differently such that transient regressors are formed by convolving stick functions of duration of TR/number of slices and amplitude number of slices/TR with a basis set. By contrast, epoch regressors are formed by convolving box cars of duration equal to the event and amplitude of 1 with a basis set. These conventions result in parameter estimates that are scaled differently for transient and epoch events. Thus, to directly compare the transient and sustained fMRI phases, we z-scored activations within a given phase before statistical analysis. While z-scoring puts each phase on the same scale, it also centers the data such that positive activations can correspond to a negative z score if such positive activations are below the overall mean. So as not to give false impressions of the sign of activations, and purely for visualization purposes, see Figure 4 for depiction of the data without z-scoring. All statistical tests comparing transient and sustained phases are done with z-scored data as described above.

In keeping with our past work (Nee and D'Esposito, 2016, 2017; Nee, 2021), for other analyses, we focused on data collected during the subtask phase as this phase most clearly distinguishes the different control

Table 1. ROI coordinates (MNI)

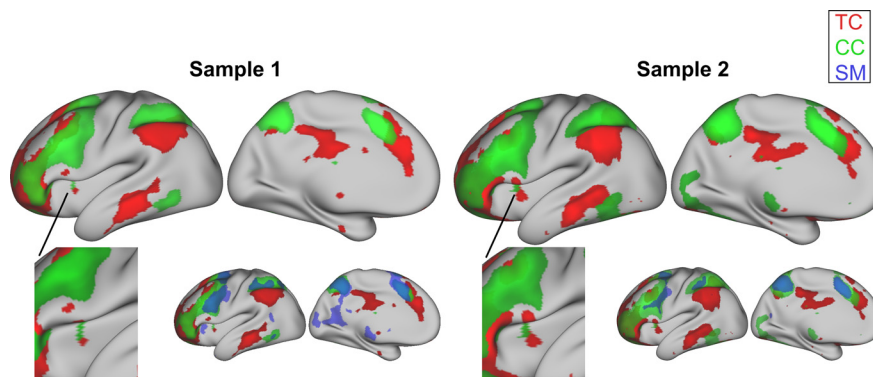|	Sample 1			Sample 2		
	x	*y*	*z*	*x*	*y*	*z*
CC dmPFC	−6	18	46	−6	18	48
TC dmPFC	−8	38	32	−4	38	36
CC al	−28	24	0	−28	24	0
TC al	−32	18	−6	−32	18	−8

Figure 2. Activation maps. Main effects of temporal control (TC; red) and contextual control (CC; green) overlaid, shown for each sample. Inset, close-up view of anterior insula. Because of overlap between contextual and sensory-motor (SM) contrasts (blue, bottom) within the CON, contextual control activations are displayed alongside temporal control, while all control-related activations are shown for comparison below with sensory-motor color in blue (sensory-motor control activations were assessed by an interaction contrast; for full details, see Materials and Methods). Threshold was set at $t = 2.3$ for visualization purposes; L hemisphere is shown.

processes. Where appropriate, the normality of the data was tested using Shapiro–Wilk tests, and Mauchly's test of sphericity was used to test for equal variance. When normality was violated (Shapiro–Wilk tests, $p < 0.05$), Wilcoxon-corrected values are reported (denoted by p_{w}) and effect sizes (r) were calculated using the formula $r = z/\text{square root}(N)$ (Fritz et al., 2012). Mauchly's test of sphericity was met as all analyses had only two levels within factors and therefore only one set of difference scores.

Multidimensional scaling. Following our past work (Nee, 2021), ROI data were submitted to multidimensional scaling. Individual-level ROI data were z-scored across conditions and compiled into a two-dimensional matrix, as follows: one dimension of individuals × condition, and another dimension of ROIs. A dissimilarity matrix based on the ROIs was calculated using $1 − r$, where r is the Pearson's correlation and submitted to the MATLAB cmdscale function. ROIs were plotted as a point in space defined by the resultant first three dimensions.

To examine clustering within the space formed by multidimensional scaling, we calculated average Euclidean distance within and between clusters. We explored several different methods of defining clusters including defining clusters as a function of the cognitive control demands that defined the ROIs (i.e., temporal control vs contextual control), by network (i.e., FPN vs CON), and by combinations of these [i.e., FPN areas responsive to TC (FPN_{TC}) vs CON areas sensitive to TC (CON_{TC}), FPN areas responsive to CC (FPN_{CC}) vs CON areas sensitive to CC (CON_{CC})]. The ratio of between-cluster versus within-cluster distance was compared with a null distribution formed by randomly permuting ROI labels (i.e., shuffling the ROIs among control demand and network) 5000 times to determine significance.

Repeated-measures correlations and mediation analysis. Behavioral data were analyzed as in Nee (2021), with repeated-measures correlations calculated in the rmcorr package of R (Bakdash and Marusich, 2017). Mean reaction time (RT) from each of the eight conditions was calculated and z-scored by individual separately for the subtask and return trials, whereas the fMRI activation from each ROI was drawn from the subtask phase only for these analyses. To obtain results of present behavior, RT during subtask trials was correlated with activation during

the subtask phase while partialing out RT during return trials. Future behavior involved correlating RT during the return trial with subtask phase fMRI data while partialing out RT during subtask trials. These procedures were performed separately for each sample. Statistical significance was assessed after Bonferroni correction for the number of ROIs.

Mediation analyses were implemented using the bmlm package in R as described in the study by Vuorre and Bolger (2018). This package models Bayesian multilevel mediation analyses for use in within-subjects designs using Monte Carlo procedures from underlying Stan software to fit the model. The variables input into the model included average ROI estimates as predictors and z-scored RTs from present or future trials depending on the subnetwork analysis. Analyses involving present behavior controlled for return trial RTs, while analyses involving future behavior controlled for subtask trial RTs. Subnetwork variates were created by averaging activations across ROIs of a given subnetwork.

Results

Cognitive control demand distribution in the cingulo-opercular network

Prior research of the FPN has documented functional variation along a somatomotor–proximal to somatomotor–distal axis (Dixon, 2018; Murphy et al., 2020; Nee, 2021; Abdallah et al., 2022). In the lateral PFC, this axis has been described in terms of abstraction of cognitive control (Badre, 2008; Badre and Nee, 2018) with several accounts detailing that such abstraction can be quantified as a function of the timescales over which cognitive control operates (Fuster, 2001; Koechlin et al., 2003; Koechlin and Summerfield, 2007). The axis observed in the lateral PFC is also mirrored in the posterior parietal cortex (Choi et al., 2018; Nee, 2021), suggesting that functional descriptions that apply to the lateral PFC are actually a reflection of the broader FPN. However, temporal abstraction has not always been sufficient to properly describe gradients within the FPN (Reynolds et al., 2012; Nee et al., 2014; Badre and Nee, 2018; Pitts and Nee, 2022). Previously, we suggested that a more generalizable principle may be gained by noting the connections of gradients within the FPN, and of networks that lie on either end of the axis: namely, the dorsal attention network on the somatomotor proximal end and the default mode network on the somatomotor distal end (Nee, 2021). Somatomotor proximal areas of the FPN are then well positioned to support control over externally driven stimuli in the present moment, while somatomotor distal areas of the FPN are well positioned to support control over internally generated representations that prepare for the future.

Here we examined the extent to which similar principles can be applied to the CON. We analyzed control demand contrasts that isolate effects of sensory-motor control-selecting the appropriate action based on a stimulus; contextual control-selecting the context-appropriate task set; and temporal control-sustaining an internal representation to guide future cognition (see Materials and Methods). Collectively, these control processes form an external–present to internal–future axis.

Whole-brain contrasts of the effect of temporal control showed peak activation in a rostral region of the dmPFC (Table 1; Fig. 2, red; sample 1, −8, 38, 32; sample 2, −4, 38, 36). By contrast, both contextual (Fig. 2, green; sample 1, −6, 18, 46; sample 2, −6, 18, 48) and sensory-motor control (Fig. 2, blue; sample 1, −4, 18,
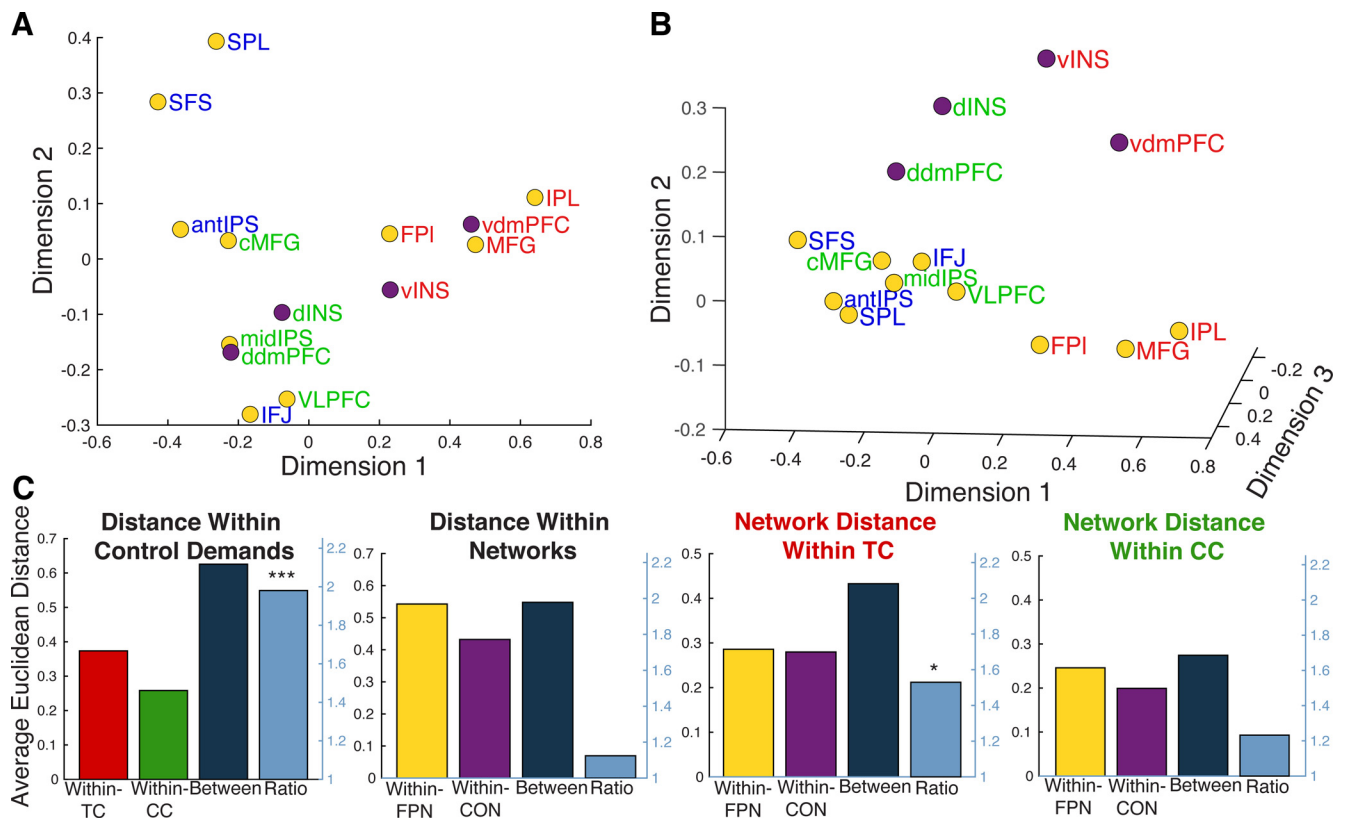
Figure 3. Multidimensional scaling between networks. ***A***, First two dimensions resulting from multidimensional scaling of the activation profiles across regions show the CON regions (purple circles) plotted similarly to FPN (yellow circles) and clustered based on the control demands, which defined the ROIs (red font, temporal control; green font, contextual control; blue font, sensory-motor control). ***B***, The addition of the third dimension demonstrating the separation among CON and FPN regions. ***C***, Average Euclidean distance of ROIs within control demands, networks, and subnetworks, exhibiting larger differences between control/network (dark blue) than within. Significance of this ratio (light blue, right axis) was tested against a null distribution. *$p < 0.05$, ***$p < 0.001$.

48; sample 2, −6, 12, 52) contrasts revealed a more caudal dmPFC peak that was similar across contrasts. The aI showed similar separations with a distinct ventral-most region active for temporal control (Fig. 2, red; sample 1, −32, 18, −6; sample 2, −32, 18, −8), and a more dorsal region active for contextual (Fig. 2, green; sample 1, −28, 24, 0; sample 2, −28, 24, 0) and sensory-motor control (Fig. 2, blue; sample 1, −28, 28, 2; sample 2, −26, 28, 0). These data suggest that both the dmPFC and aI are topographically organized by control demand with more ventral areas sensitive to more abstract temporal control, and more dorsal areas sensitive to more concrete forms of control. Given the close correspondence among CON peak activations in the contextual and sensory-motor control contrasts, peaks defined by contextual control were used in follow-up ROI analyses.

Contrasts provide a hypothesis-driven way to reduce the dimensionality of the data and reveal dissociations among brain areas. It is often useful to supplement such hypothesis-driven approaches with more data-driven approaches. Previous work used multidimensional scaling on activations across the eight conditions of interest in areas of the FPN to provide a data-driven method of examining dissociations within the FPN (Nee, 2021). Those data revealed that the FPN could be classed along two dimensions—a primary dimension reflecting abstraction of control with concrete/somatomotor proximal areas at one end and abstract/somatomotor distal areas at the other, and a second dimension reflecting stimulus domain with ventral/ verbal areas at one end and dorsal/spatial areas at the other. Those dimensions resembled the principle macroscale gradients of cortex (Mesulam, 1998; Margulies et al., 2016; Huntenburg et al., 2018), but detailed within the FPN. To examine whether

CON areas align similarly, we added our 4 CON ROIs to the 10 FPN ROIs previously examined (Nee, 2021) and repeated the multidimensional scaling.

We hypothesized that one of the following two patterns would emerge: (1) CON areas would cluster together, resembling a distinct network from the FPN, but would show their own dimensional pattern; or (2) CON areas would group with FPN areas of a similar functional preference (e.g., CON temporal control areas would group with FPN temporal control areas). Aggregating ROIs from both CON and FPN, two dimensions captured 77% of the variance of the data. As depicted in Figure 3A, CON areas intermingled with FPN areas in a control-specific manner: areas defined by temporal control in both networks (red) clustered together and were spatially distinct from areas defined by contextual control (green). When a third dimension was added, the variance explained increased to 86%, and the CON and FPN were clearly delineated from one another while maintaining their functional segregation (Fig. 3B).

To quantify these clusterings, we calculated the average Euclidean distance of areas as a function of control demand (temporal control, contextual control), network (FPN, CON), and the combination of these factors (Fig. 3C). We created a null distribution formed by randomly shuffling ROI labels 5000 times. The ratio of the average between-cluster versus within-cluster distance in the true data was compared with the same ratio in the null distribution. Confirming the visual impressions in Figure 3, A and B, the average distance among areas defined by a control demand (temporal control, 0.37; contextual control, 0.26) was less than the average distance between areas defined by distinct control demand (between
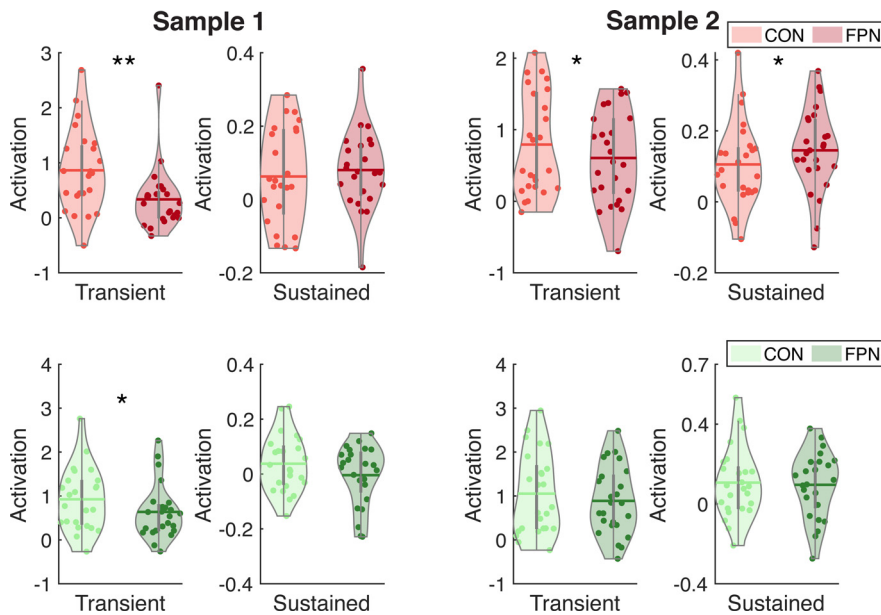
Figure 4. Transient versus sustained analysis. Average activations from the CON and FPN subnetworks during transient and sustained phases, samples shown separately. Red distributions represent the temporal control subnetwork, and green distributions represent the contextual control subnetwork. Lighter shades, CON; darker shades, FPN. Mean values are depicted by horizontal lines. $*p < 0.05$, $**p < 0.001$.

temporal and contextual control regions, 0.63). The between-cluster versus within-cluster ratio was highly significant ($p < 0.0002$), indicating that areas grouped within control demand were generally closer in the multidimensional scaling space than areas that spanned different control demands. Likewise, the within-network distance was numerically smaller (FPN, 0.54; CON, 0.43) when compared with the between-network average distance (0.55); however, this clustering did not achieve significance ($p = 0.07$). When jointly considering both control demand and network, we found significant clustering by network within areas sensitive to temporal control (FPN$_{TC}$ distance, 0.29; CON$_{TC}$ distance, 0.28; between areas, 0.43; $p = 0.042$). A similar numerical trend was not significant within areas sensitive to contextual control (control FPN$_{CC}$ distance, 0.25; CON$_{CC}$ distance, 0.20; between, 0.27; $p = 0.16$). These data indicate that the FPN and CON fractionate primarily as a function of cognitive control demands. Fractionations by network were present, but more subtle. These data are consistent with the idea that both the FPN and CON group together across diverse cognitive demands as a multiple demand system (Duncan, 2010), that this system can be fractionated along a gradient of cognitive demands (Dixon et al., 2018; Murphy et al., 2020; Nee, 2021; Abdallah et al., 2022), and, within these gradients, that there are also fractionations by network.

Collectively, the whole-brain and multidimensional scaling results indicate that the CON fractionates into subnetworks based on control demands, similar to those of the FPN. Furthermore, there was evidence for functional separation of the CON and FPN. Hence, areas in the CON and FPN align by control function, but fractionate by network. To examine what drives these fractionations, we next contrasted transient and sustained roles of the CON and FPN.

Transient versus sustained activations
Prior literature has alternately characterized the CON as providing either phasic signals to adapt and adjust control (Botvinick et al., 2001; Menon and Uddin, 2010) or tonic signals to maintain a steady controlled state (Dosenbach et al., 2007; Sadaghiani and D'Esposito, 2015). To adjudicate among these roles, we

contrasted CON and FPN activations during transition phases of the task, which require transient adjustments, and static phases of the task, which require sustained control (see Materials and Methods; Fig. 1B). This was done separately for each CON and FPN control subnetwork by averaging across areas within a given subnetwork (e.g., ventral aI and ventral dmPFC for the CON$_{TC}$ subnetwork).

Activations for each CON and FPN subnetwork were entered into separate ANOVAs with factors of network (CON $\times$ FPN) and phase (transient $\times$ sustained). Because of differences in how SPM scales sustained and transient regressors (see Materials and Methods), parameter estimates were z-scored within a phase before statistical analysis, while non-z-scored data are used for visualization purposes to depict the fact that areas are broadly positively engaged across all demands (Fig. 4). Within areas sensitive to temporal control, we observed a significant network by phase interaction in both samples (sample 1: $F_{(1,23)} = 90.61$, $p < 0.001$; sample 2: $F_{(1,24)} = 21.65$, $p < 0.001$), indicating that the CON and FPN were differentially sensitive to transient versus sustained phases of the task. Areas sensitive to contextual control did not show an interaction effect in either sample 1 ($F_{(1,23)} = 2.74$, $p = 0.11$) or sample 2 ($F_{(1,24)} = 1.86$, $p = 0.19$).

Overall, there was a tendency for CON areas to show greater transient activations than FPN areas (transient CON$_{TC}$ vs FPN$_{TC}$: sample 1: $t_{(23)} = 5.69$, $p_w < 0.001$, $r = 0.80$; sample 2: $t_{(24)} = 2.38$, $p_w = 0.02$, $r = 0.47$; transient CON$_{CC}$ vs FPN$_{CC}$: sample 1: $t_{(23)} = 2.78$, $p_w = 0.03$, $r = 0.45$; sample 2: $t_{(24)} = 1.18$, $p_w = 0.35$, $r = 0.19$). By contrast, within areas sensitive to temporal control, sustained FPN activations were numerically larger than sustained CON activations, although this difference was only significant in sample 2 (sustained CON$_{TC}$ vs FPN$_{TC}$: sample 1: $t_{(23)} = -0.82$, $p_w = 0.59$, $r = 0.11$; sample 2: $t_{(24)} = -2.56$, $p_w = 0.03$, $r = 0.44$). The reverse was true in areas sensitive to contextual control as these tended to show more numerically, though not significantly, greater sustained activation in the CON relative to FPN (sustained CON$_{CC}$ vs FPN$_{CC}$: sample 1: $t_{(23)} = 2.02$, $p_w = 0.08$, $r = 0.36$; sample 2: $t_{(24)} = 0.38$, $p_w = 0.60$, $r = 0.11$).

Based on these results, we considered whether the overall CON > FPN effects were because of increased signal-to-noise ratio (SNR; i.e., the midline regions of the CON may be improved more by smoothing compared with the lateral regions of the FPN, leading to higher signal and differentially higher activation patterns). To control for this possibility, we computed temporal SNR for each CON and FPN region and regressed this out of our data to reanalyze the factors. The results broadly replicated the above, with the addition of the interaction effect of CC in sample 1 becoming significant because of greater CON activation in the transient versus sustained phases ($F_{(1,23)} = 6.97$, $p = 0.01$). These results suggest that the observed effects are not because of differences in SNR across regions.

These results suggest that the temporal roles of the CON versus FPN are qualified by their functional subnetworks. Although areas within both networks are broadly active in both transient
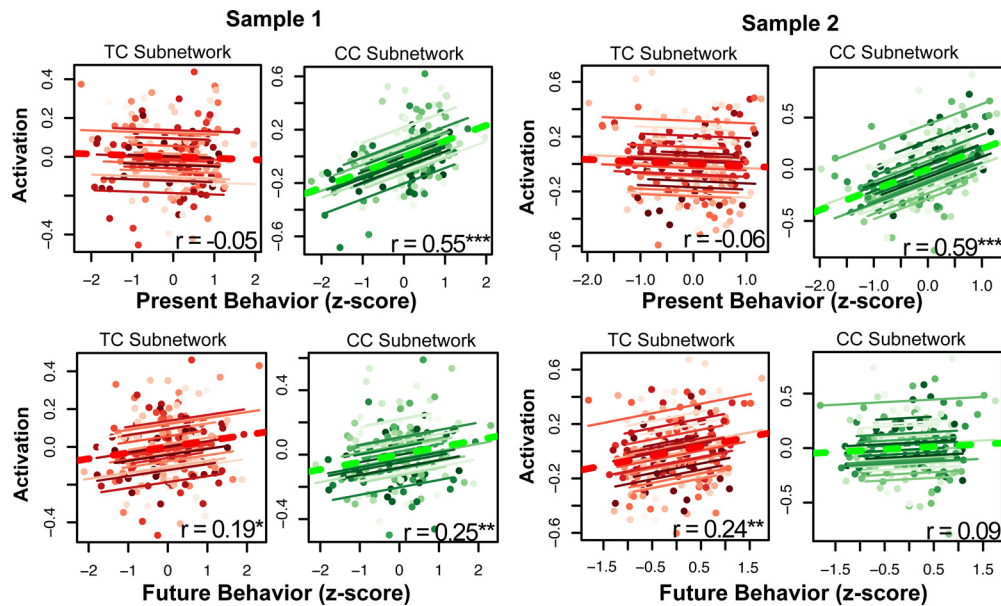
Figure 5. CON subnetwork correlation with behavior. Repeated-measures correlations among average CON subnetwork activation, z-scored current trial RT (present behavior), and z-scored return trial RT (future behavior). TC subnetworks show positive correlations with future behavior across samples (controlling for present behavior), and CC subnetworks are positively correlated with present behavior (controlling for future behavior) across samples. Parallel solid lines represent fit to the data from separate subjects, with the group mean plotted as the dashed line per subnetwork. $*p < 0.05$, $**p < 0.01$, $***p < 0.001$.

and sustained phases of the task, the CON tended to be more active than FPN in general. An exception to this rule was observed within areas sensitive to temporal control wherein the FPN had a tendency to be as active or more active than the CON during sustained phases of the task. However, what remains unclear is how these networks interact to support cognitive control. We turn to this question next.

Directional relationship from the cingulo-opercular network to behavior

Prior work has suggested that parallel medial-to-lateral PFC systems are organized by a control process whereby medial areas send motivational incentives to lateral areas to exert top-down control (Kouneiher et al., 2009). Alexander and Brown (2018) computationally formalized and extended this idea, suggesting that signals from parallel medial-to-lateral PFC areas reflect prediction errors more broadly that serve to update lateral PFC representations. Based on these works, we hypothesized that the role of the medial PFC may extend to the CON more generally, and the role of the lateral PFC may extend to the FPN more generally. If so, one would predict that the CON drives the FPN, which, in turn, drives controlled behavior.

To test this idea, we began by examining the relationship of each subnetwork to behavior. Following previous work (Nee and D'Esposito, 2016, 2017; D'Mello et al., 2020; Nee, 2021), we separately characterized present and future behavior, respectively. We focused on neural signals during subtask phases wherein cognitive control demands were manipulated, while varying the phase of the behavior of interest. Present behavior was calculated as the average reaction time during subtask trials for a particular condition for a particular individual. Future behavior was calculated as the average reaction time for return trials for a particular condition for a particular individual. Then, individual/condition-specific activations during the subtask trials (i.e., sustained phase) were related to present behavior while partialing out contributions of future behavior, and future behavior while partialing out contributions of present behavior. The logic of this analysis is that

present behavior reflects behavior at the same time at which the neural signals are measured (i.e., both are during the sustained, subtask phase). Future behavior reflects behavior for which sustained, subtask signals are preparing. Hence, activations that correlate with future behavior, but not present behavior, indicate activations that prepare control for the future, but do not act in the moment. Activations that correlate with present behavior, but not future behavior, indicate activations that reflect control in the moment. In previous work, we found that within the FPN, the temporal control subnetwork correlates with future, but not present behavior, the sensory-motor control subnetwork correlates with present, but not future behavior, and the contextual control subnetwork correlates with both (Nee and D'Esposito, 2016, 2017; Nee, 2021). That is, increasingly sensory-motor distal areas are increasingly future oriented.

To examine whether the CON subnetworks also related to present or future behavior, we examined the relationship of CON activations to present and future behavior through repeated-measures correlations with RT (Fig. 5). The CON_{CC} subnetwork showed a significant positive correlation with present behavior across samples [sample 1: $r = 0.55$; confidence interval (CI), (0.43, 0.64); $p < 0.001$; sample 2: $r = 0.59$; CI, (0.48, 0.68); $p < 0.001$], as well as with future behavior in sample 1 to a lesser degree [$r = 0.25$; CI, (0.10, 0.39); $p = 0.001$; sample 2: $r = 0.09$; CI, (−0.06, 0.23); $p = 0.24$]. In comparison, the CON_{TC} subnetwork was not correlated with present behavior in either sample [sample 1: $r = −0.05$, CI, (−0.20, 0.11); $p = 0.56$; sample 2: $r = −0.06$, CI, (−0.20, 0.09); $p = 0.45$], but was positively correlated with future behavior in both samples [sample 1: $r = 0.19$; CI, (0.04, 0.33); $p = 0.01$; sample 2: $r = 0.24$; CI, (0.10, 0.38); $p = 0.001$]. Collectively, these data are consistent with prior patterns observed in the FPN—areas defined by temporal control tend to be future oriented, but not present oriented, while areas defined by contextual control tend to reflect both current and future control demands. However, given that for the CON_{CC} subnetwork the relationship to future behavior was not consistent across samples, we focus on its relationship to present behavior in subsequent analyses.
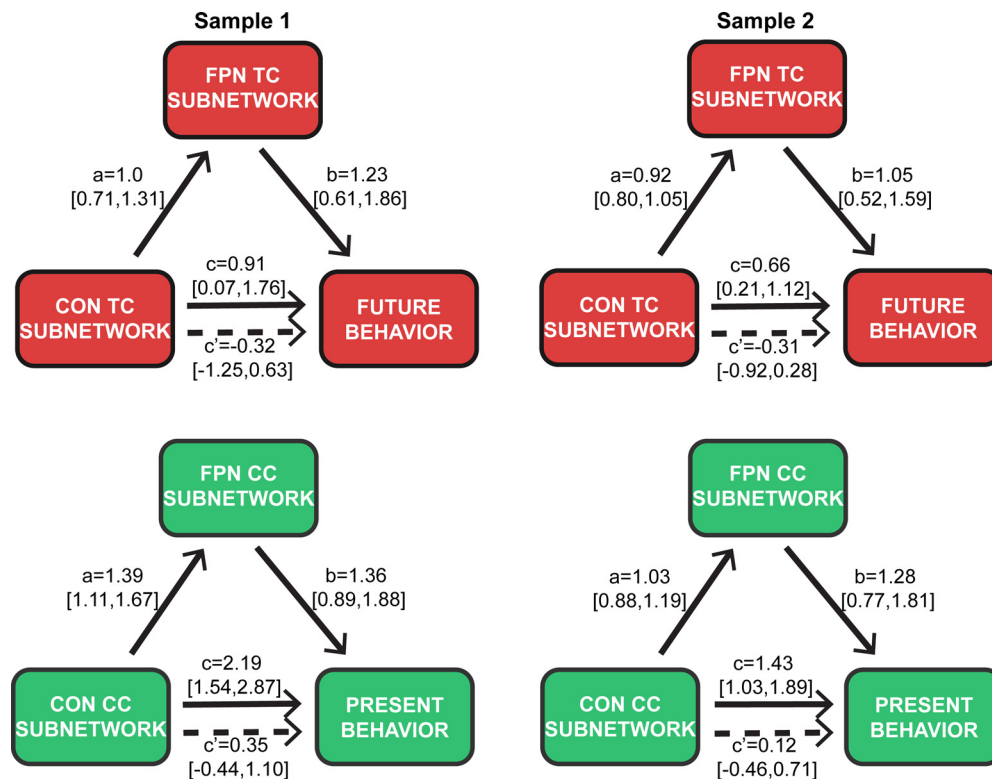
Figure 6. CON to FPN mediation with behavior. Each CON subnetwork's relationship with behavior is mediated by the respective FPN subnetwork. Red models show temporal control subnetwork mediation analysis with future behavior (*z*-scored future trial RT) based on correlation results shown in Figure 5. Green models show contextual control subnetwork mediation with present behavior (*z*-scored current trial RT). Across samples the direct path (*c*) from the CON to behavior became insignificant (*c′*) after adding in the FPN activation mediator to the model. Point estimates from each path shown with 95% CI. The indirect effect (*c′*) is considered significant if the CI does not overlap with zero.

Having established that distinct subnetworks of the CON relate to distinct aspects of controlled behavior in similar ways as the FPN, we next moved to test the hypothesis that the CON drives the FPN, which, in turn, drives controlled behavior. We used a set of mediation analyses to quantify the extent to which each network affects another. We hypothesized that if the CON drives the FPN, which drives behavior, then the FPN should mediate the relationship between the CON and behavior.

Separate mediation analyses were computed among the CON_{CC} and FPN_{CC} subnetworks and present behavior, as well as CON_{TC} and FPN_{TC} subnetworks and future behavior, respectively (Fig. 6). In each case, we found evidence for a full mediation across both of the following samples: areas defined by contextual control [sample 1: $c = 2.19$; 95% CI, (1.54, 2.87); $c′ = 0.35$; 95% CI, (−0.44, 1.10); proportion-mediated effect, 85%; 95% CI, (0.54, 1.24); sample 2: $c = 1.43$; 95% CI, (1.03, 1.89); $c′ = 0.12$; 95% CI, (−0.46, 0.71); proportion-mediated effect, 93%; 95% CI, (0.55, 1.37)]; and areas defined by temporal control [sample 1: $c = 0.91$; 95% CI, (0.07, 1.76); $c′ = −0.32$; 95% CI, (−1.25, 0.63); sample 2: $c = 0.66$; 95% CI, (0.21, 1.12); $c′ = −0.31$; 95% CI, (−0.92, 0.28)]. To better solidify the directionality of this result, we repeated the analyses, but with the roles of the CON and FPN switched (i.e., CON mediates the relationship between the FPN and behavior). No analysis demonstrated a mediation effect by the CON ($c′$, CI did not include zero). These results are consistent with the idea that the CON motivates the FPN, which, in turn, drives behavior. Furthermore, they indicate that this general pattern is observed across subnetworks defined by distinct forms of control (temporal, contextual) at distinct behavior timescales (future, present).

Thus far, we have treated subnetworks of the CON collectively, ignoring potential functional differences between the

dmPFC and aI. Signals in the dmPFC and aI are often highly correlated, making it difficult to tease apart distinct functional roles of each region (but see Magno et al., 2006). However, neuroanatomically, the aI is synaptically close to sensory areas and serves as a hub for both exteroceptive and interoceptive sensory signals (e.g., olfaction, gustation, and pain; Mufson and Mesulam, 1982; Flynn, 1999; Wang et al., 2019), while the dmPFC is synaptically close to motor areas (Picard and Strick, 1996, 2001; Beckmann et al., 2009). This suggests that within the CON, the aI may be considered more of an input zone whereas the dmPFC may be considered more of an output zone (or afferent and efferent zones; Seeley, 2019). If so, there may be directionality within the CON itself such that the aI drives the dmPFC, which, in turn, drives the FPN.

To test this hypothesis, we ran a series of models to test for mediation within the CON and between the CON and FPN. Our first analysis modeled the dmPFC mediating the aI relationship with the FPN, followed by an analysis of the FPN mediating the dmPFC relationship with behavior. If this progression shows mediated effects on the aI and dmPFC, this would be consistent with the hypothesis that the CON relationship to behavior occurs from the aI, to dmPFC, and through the FPN. Once again, we separated the control subnetworks with their respective behavioral results: the temporal control subnetwork relationship with future behavior and the contextual control subnetwork relationship with present behavior. Results are shown in Figure 7. Within the temporal control subnetwork, the aI_{TC} to FPN_{TC} relationship was mediated by the $dmPFC_{TC}$ across samples [sample 1: $c = 0.72$; 95% CI, (0.47, 0.97); $c′ = 0.37$; 95% CI, (0.14, 0.62); proportion-mediated effect, 48%; 95% CI, (0.16, 0.78); sample 2: $c = 0.74$; 95% CI, (0.54, 0.93); $c′ = 0.13$; 95% CI, (−0.07, 0.34); proportion-mediated effect, 83%; 95% CI, (0.59, 1.11)]. Likewise, the $dmPFC_{TC}$
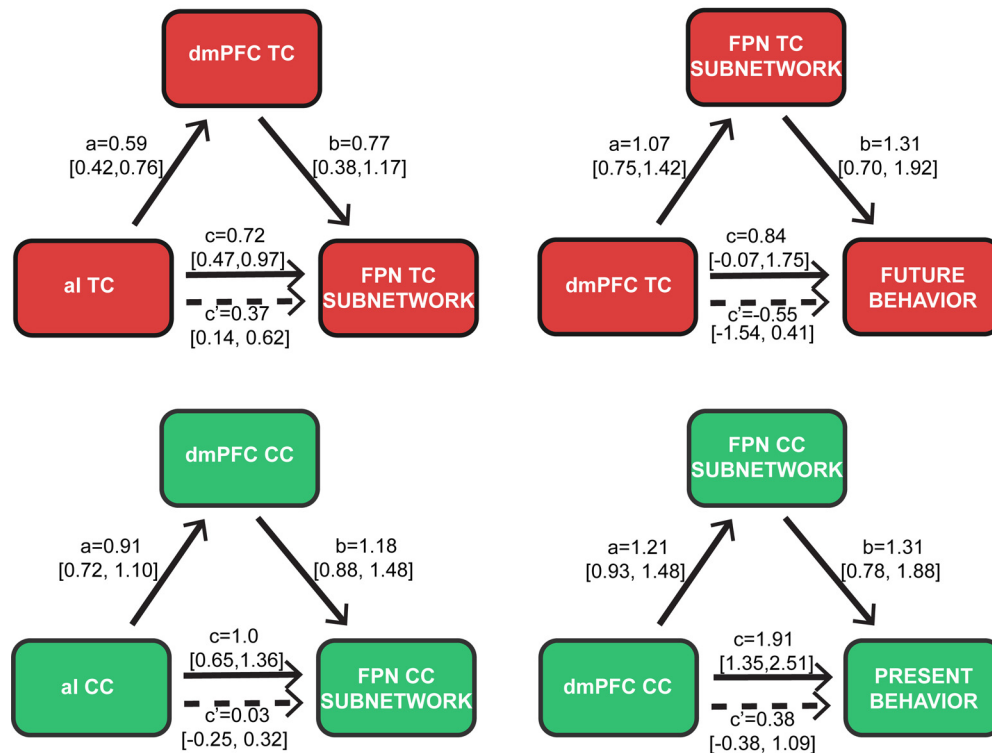
Sample 1

Figure 7. Within CON to FPN to behavior mediation analysis. Within the CON, the dmPFC mediates the relationship between the aI and FPN. In turn, the FPN mediates the relationship between the dmPFC and behavior. Such data are consistent with aI-to-dmPFC-to-FPN chains guiding behavior in a motivation-to-control-to-action motif. Results are separated by functional subnetworks and related behavioral measure (present behavior for CC and future behavior for TC). Sample 1 data are shown, and all effects are replicated in sample 2 and reported in the main text.

relationship to future behavior was mediated by the FPN_{TC} [sample 1: $c = 0.84$; 95% CI, $(-0.07, 1.75)$; $c' = -0.55$; 95% CI, $(-1.54, 0.41)$; sample 2: $c = 0.62$; 95% CI, $(0.27, 0.97)$; $c' = -0.03$; 95% CI, $(-0.53, 0.47)$]. In the contextual control subnetwork, there were similar effects of mediation seen in both analyses: aI_{CC} to FPN_{CC} mediated by $dmPFC_{CC}$ [sample 1: $c = 1.00$; 95% CI, $(0.65, 1.36)$; $c' = 0.03$; 95% CI, $(-0.25, 0.32)$; proportion-mediated effect, 99%; 95% CI, $(0.72, 1.32)$; sample 2: $c = 1.09$; 95% CI, $(0.87, 1.31)$; $c' = 0.25$; 95% CI, $(-0.02, 0.51)$; proportion-mediated effect, 78%; 95% CI, $(0.57, 1.02)$], and $dmPFC_{CC}$ to present behavior mediated by FPN_{CC} [sample 1, $c = 1.91$; 95% CI, $(1.35, 2.51)$; $c' = 0.38$; 95% CI, $(-0.38, 1.09)$; proportion-mediated effect, 81%; 95% CI, $(0.47, 1.24)$; sample 2: $c = 1.13$; 95% CI, $(0.82, 1.47)$; $c' = 0.26$; 95% CI, $(-0.16, 0.71)$; proportion-mediated effect, 77%; 95% CI, $(0.42, 1.16)$]. These analyses are consistent with a directional interaction between the CON and FPN networks that can be further tested using causal methodologies (see Discussion). In particular, the analyses are consistent with a model wherein the CON subnetworks motivate the respective FPN subnetworks on behavior. This process can be further broken down within the CON such that the aI directs the dmPFC toward the FPN.

Discussion

The present study examined the functional roles and interactions among the FPN and CON during a comprehensive control task. As we previously observed within the FPN (Nee and D'Esposito, 2016, 2017; Nee, 2021), the CON fractionated as a function of control demands along an external/present-oriented to internal/future-oriented axis. Ventral areas within the dmPFC and aI preferentially responded to temporal control, requiring sustaining an internal

representation for the future. Dorsal areas within the dmPFC and aI preferentially responded to conditions requiring selecting actions according to stimuli and context-specific task sets (sensory-motor control and contextual control, respectively). Functional activation patterns revealed that areas across the CON and FPN could be grouped principally as a function of control demand (i.e., temporal control vs contextual control), and secondarily as a function of network (CON, FPN), suggesting that both the CON and FPN contain functional subnetworks that support distinct forms of control. Furthermore, we found evidence that the CON was consistently more engaged than the FPN during transitions into and out of specific modes of control, indicating an important role in transient processes that may adapt control. By contrast, we found some evidence that FPN areas responsive to temporal control (FPN_{TC}) show more of a sustained role. Finally, we found that, as in the FPN, CON areas sensitive to contextual control (CON_{CC}) were correlated with present behavior, while CON areas sensitive to temporal control (CON_{TC}) were correlated with future behavior. These relationships were mediated by respective FPN subnetworks consistent with the idea that the CON motivates the FPN, which, in turn, drives behavior. Moreover, within the CON, the dmPFC mediated the relationship between the aI and FPN, suggesting that the dmPFC acts as the crux linking the CON to the FPN. Collectively, these data indicate that parallel CON–FPN subnetworks mediate controlled behaviors at distinct timescales.

Timescale in the CON

Our work sheds light on the conflicting explanations of the CON function throughout the literature. Previous theories have

provided opposing accounts of whether the CON is primarily involved in transient processing [e.g., dynamic between-network switching (Menon and Uddin, 2010), conflict detection (Botvinick et al., 2001), and signaling prediction errors (Alexander and Brown, 2011)], or sustained processing [e.g., sustaining task sets (Dosenbach et al., 2006, 2007, 2008) and vigilance (Sadaghiani and D'Esposito, 2015)]. Additionally, a sustained role of the CON is supported by findings that the intrinsic neural timescales of the ACC, which is within the CON, is highest among cortical areas (Murray et al., 2014; Chaudhuri et al., 2015; for review, see Cavanagh et al., 2020). Our results show evidence for the CON operating in both roles. During transitions into and out of control modes, the CON showed consistently greater activation than the FPN, suggesting a role in transient processing. However, in areas sensitive to contextual control, the CON also tended to show greater sustained activations than the FPN, suggesting a sustained role. Notably, this sustained pattern was reversed in areas sensitive to temporal control wherein FPN areas tended to be more active than the CON areas. Collectively, these data suggest that some discrepancies in past work may result from examining areas in different subnetworks. In comparison to the FPN, examining areas relevant to contextual control would suggest that the CON acts in a more sustained manner, while examining areas relevant to temporal control would suggest that the CON acts in a more transient manner. Our data indicate that both modes of operation are true, but that, for control processing involving sustaining internal representations (temporal control), the FPN seems more strongly tied to sustained processing.

CON and FPN interactions

That the CON is particularly responsive to transient changes aligns with numerous models proposing that CON regions act as motivators toward the FPN. Previous work has detailed this framework through a parallel rostrocaudal axis in the medial PFC, mirroring the lateral PFC (Kouneiher et al., 2009; Venkatraman et al., 2009; Taren et al., 2011; Alexander and Brown, 2018). Importantly, much of the work suggesting the motivational account of the CON, and more specifically the ACC, has demonstrated motivation through reward or value incentive (Kouneiher et al., 2009; Shenhav et al., 2013). Our results add to these findings by outlining a potentially directed output of behavior from the medial to lateral regions of the PFC during control without explicit reward incentives. Critically, we provide empirical evidence consistent with directional interactive roles, building on previous work of the medial to lateral PFC interactions. Using the selective relationship of each subnetwork with behavior, our results show that the activation of CON toward behavior is mediated by the respective FPN subnetwork.

Internal–external axes in the FPN and CON

Recent work has detailed a separation of large-scale networks into more precise and functionally relevant subnetworks. For example, within the Yeo et al. (2011) 17-network parcellation, the FPN fractionates into three subnetworks. Follow-up work has revealed that somatomotor proximal areas of the FPN respond to more present/externally oriented control and tend to interact with more attention-oriented and sensory-oriented brain networks (Dixon et al., 2018; Murphy et al., 2020; Nee, 2021). By contrast, somatomotor distal areas of the FPN respond to more future and internally oriented control and tend to interact with networks involved in internal mentation (e.g., DMN).

Within the CON there is less consensus. Many functional studies aggregate the cingulo-opercular regions into a single network (e.g., the ventral attention/salience network in the Yeo et al.

(2011) 7-network parcellation), while other whole-brain parcellations differentiate the regions into distinct dorsal–caudal and ventral–rostral networks (Power et al., 2011; Yeo et al., 2011; Gordon et al., 2016; Gratton et al., 2018), the functional roles of which are unclear (for review, see Gratton et al., 2018; Menon and D'Esposito, 2021). Here, we find that the same control demands that fractionate the FPN also fractionate the CON. Specifically, ventral–rostral aspects of the dmPFC and aI were sensitive to temporal control, while dorsal–caudal aspects of the dmPFC and aI were sensitive to contextual and sensory-motor control. Given that subnetworks within the CON have not spatially aligned across studies (Yeo et al., 2011; Gordon et al., 2016), that alignments can vary as a function of task demands (Salehi et al., 2020; Dworetsky et al., 2021), and that the CON itself can align with distinct other networks as a function of control demands (Cocuzza et al., 2020), it is difficult to precisely map the present findings onto existing network parcellations. Nevertheless, the collective data indicate that the CON does fractionate along a dorsal–caudal/ventral–rostral axis, which has marked parallels to the external–present/internal–future axis we have observed in the FPN (Nee, 2021).

These results may facilitate reformatting our definition of the functions of CON areas, particularly with respect to a putative role in computing salience (Seeley, 2019). On the one hand, salience is often thought of as sensory phenomenon as stimuli that tend to draw visuospatial attention (Jonides and Yantis, 1988; Theeuwes, 1993). Consistent with this, the more dorsal–caudal salience/ventral attention network of the Yeo-17 atlas includes the temporoparietal junction and inferior frontal cortex, which form the classic "bottom-up attention" network (Corbetta and Shulman, 2002). On the other hand, salience can arise as a function of personal experiences such that certain stimuli acquire affective significance (e.g., reward, threat). Consistent with this, multiple studies have detailed an internal salience component, including the original work from Seeley et al. (2007), wherein salience was defined based on prescan anxiety scores (see also, Uddin, 2015; Wang et al., 2019). Notably, the salience network includes areas associated with reward (ventral tegmental area) and affect (amygdala). The connection to these affective structures would place this latter internal salience network in line with the "internal milieu" as detailed in the study by Mesulam (1998). Together, we propose that the more dorsal–caudal areas of the aI and dmPFC are part of an externally oriented salience network, while the more ventral–rostral areas of the aI and dmPFC are part of an internally oriented salience network, paralleling the axis observed in the FPN (Nee, 2021).

Future directions

Here, we have presented evidence suggesting that serial aI to dmPFC to FPN to behavior subnetworks support distinct timescales of control. Although suggestive, directionality in the present work is limited to the inferential limits of statistical mediation. Future work using effective connectivity of the directional neuroanatomic model would further solidify these interactions within and between networks. Likewise, time-resolved techniques would aid in specifying the moment-to-moment processing, providing further insight into the transient effects of the CON and the sustained effects of the FPN temporal control subnetwork. Moreover, direct causal evidence using interventions (e.g., brain stimulation) would further bolster directional and time-dependent claims. The CON-to-FPN interactions provide evidence for a motivational framework of control that can be further tested and specified to expand knowledge on the

continuous interplay between regions that give rise to complex cognitive processing. Finally, the experimental design confounded timescale (present–future) and medium (external–internal). In the discussion above, we have vacillated between these characterizations. However, it is plausible that different aspects of control vary by time versus medium. Paradigms that deconfound these factors would help resolve such matters.

References

Abdallah M, Zanitti GE, Iovene V, Wassermann D (2022) Functional gradients in the human lateral prefrontal cortex revealed by a comprehensive coordinate-based meta-analysis. Elife 11:e76926.

Alexander WH, Brown JW (2011) Medial prefrontal cortex as an action-outcome predictor. Nat Neurosci 14:1338–1344.

Alexander WH, Brown JW (2018) Frontal cortex function as derived from hierarchical predictive coding. Sci Rep 8:3843.

Andersson JLR, Hutton C, Ashburner J, Turner R, Friston K (2001) Modeling geometric deformations in EPI time series. Neuroimage 13:903–919.

Badre D (2008) Cognitive control, hierarchy, and the rostro–caudal organization of the frontal lobes. Trends Cogn Sci 12:193–200.

Badre D, Nee DE (2018) Frontal cortex and the hierarchical control of behavior. Trends Cogn Sci 22:170–188.

Bakdash JZ, Marusich LR (2017) Repeated measures correlation. Front Psychol 8:456.

Beckmann M, Johansen-Berg H, Rushworth MFS (2009) Connectivity-based parcellation of human cingulate cortex and its relation to functional specialization. J Neurosci 29:1175–1190.

Botvinick MM, Braver TS, Barch DM, Carter CS, Cohen JD (2001) Conflict monitoring and cognitive control. Psychol Rev 108:624–652.

Braga RM, Buckner RL (2017) Parallel interdigitated distributed networks within the individual estimated by intrinsic functional connectivity. Neuron 95:457–471.e5.

Cavanagh SE, Hunt LT, Kennerley SW (2020) A diversity of intrinsic timescales underlie neural computations. Front Neural Circuits 14:615626.

Charron S, Koechlin E (2010) Divided representation of concurrent goals in the human frontal lobes. Science 328:360–363.

Chaudhuri R, Knoblauch K, Gariel M-A, Kennedy H, Wang X-J (2015) A large-scale circuit mechanism for hierarchical dynamical processing in the primate cortex. Neuron 88:419–431.

Choi EY, Drayna GK, Badre D (2018) Evidence for a functional hierarchy of association networks. J Cogn Neurosci 30:722–736.

Cocuzza CV, Ito T, Schultz D, Bassett DS, Cole MW (2020) Flexible coordinator and switcher hubs for adaptive task control. J Neurosci 40:6949–6968.

Corbetta M, Shulman GL (2002) Control of goal-directed and stimulus-driven attention in the brain. Nat Rev Neurosci 3:201–215.

Dixon ML, De La Vega A, Mills C, Andrews-Hanna J, Spreng RN, Cole MW, Christoff K (2018) Heterogeneity within the frontoparietal control network and its relationship to the default and dorsal attention networks. Proc Natl Acad Sci U S A 115:E3068–E3068.

D'Mello AM, Gabrieli JDE, Nee DE (2020) Evidence for hierarchical cognitive control in the human cerebellum. Curr Biol 30:1881–1892.e3.

Dosenbach NUF, Fair DA, Cohen AL, Schlaggar BL, Petersen SE (2008) A dual-networks architecture of top-down control. Trends Cogn Sci 12:99–105.

Dosenbach NUF, Visscher KM, Palmer ED, Miezin FM, Wenger KK, Kang HC, Burgund ED, Grimes AL, Schlaggar BL, Petersen SE (2006) A core system for the implementation of task sets. Neuron 50:799–812.

Dosenbach NUF, Fair DA, Miezin FM, Cohen AL, Wenger KK, Dosenbach RAT, Fox MD, Snyder AZ, Vincent JL, Raichle ME, Schlaggar BL, Petersen SE (2007) Distinct brain networks for adaptive and stable task control in humans. Proc Natl Acad Sci U S A 104:11073–11078.

Duncan J (2010) The multiple-demand (MD) system of the primate brain: mental programs for intelligent behaviour. Trends Cogn Sci 14:172–179.

Dworetsky A, Seitzman BA, Adeyemo B, Neta M, Coalson RS, Petersen SE, Gratton C (2021) Probabilistic mapping of human functional brain networks identifies regions of high group consensus. NeuroImage 237:118164.

Flynn FG (1999) Anatomy of the insula functional and clinical correlates. Aphasiology 13:55–78.

Fritz CO, Morris PE, Richler JJ (2012) Effect size estimates: current use, calculations, and interpretation. J Exp Psychol Gen 141:2–18.

Fuster JM (2001) The prefrontal cortex—an update: time is of the essence. Neuron 30:319–333.

Gordon EM, Laumann TO, Adeyemo B, Huckins JF, Kelley WM, Petersen SE (2016) Generation and evaluation of a cortical area parcellation from resting-state correlations. Cereb Cortex 26:288–303.

Gratton C, Sun H, Petersen SE (2018) Control networks and hubs. Psychophysiol 55:e13032.

Huntenburg JM, Bazin P-L, Margulies DS (2018) Large-Scale Gradients in Human Cortical Organization. Trends Cogn Sci 22:21–31.

Jonides J, Yantis S (1988) Uniqueness of abrupt visual onset in capturing attention. Perception and Psychophysics 43:346–354.

Koechlin E, Basso G, Pietrini P, Panzer S, Grafman J (1999) The role of the anterior prefrontal cortex in human cognition. Nature 399:148–151.

Koechlin E, Ody C, Kouneiher F (2003) The architecture of cognitive control in the human prefrontal cortex. Science 302:1181–1185.

Koechlin E, Summerfield C (2007) An information theoretical approach to prefrontal executive function. Trends Cogn Sci 11:229–235.

Kouneiher F, Charron S, Koechlin E (2009) Motivation and cognitive control in the human prefrontal cortex. Nat Neurosci 12:939–945.

Lund TE, Nørgaard MD, Rostrup E, Rowe JB, Paulson OB (2005) Motion or activity: their role in intra- and inter-subject variation in fMRI. Neuroimage 26:960–964.

Magno E, Foxe JJ, Molholm S, Robertson IH, Garavan H (2006) The anterior cingulate and error avoidance. J Neurosci 26:4769–4773.

Margulies DS, Ghosh SS, Goulas A, Falkiewicz M, Huntenburg JM, Langs G, Bezgin G, Eickhoff SB, Castellanos FX, Petrides M, Jefferies E, Smallwood J (2016) Situating the default-mode network along a principal gradient of macroscale cortical organization. Proc Natl Acad Sci U S A 113:12574–12579.

Menon V, D'Esposito M (2021) The role of PFC networks in cognitive control and executive function. Neuropsychopharmacology 47:90–103.

Menon V, Uddin LQ (2010) Saliency, switching, attention and control: a network model of insula function. Brain Struct Funct 214:655–667.

Mesulam M (1998) From sensation to cognition. Brain 121:1013–1052.

Miller JA, Voorhies WI, Lurie DJ, D'Esposito M, Weiner KS (2021a) Overlooked tertiary sulci serve as a meso-scale link between microstructural and functional properties of human lateral prefrontal cortex. J Neurosci 41:2229–2244.

Miller JA, D'Esposito M, Weiner KS (2021b) Using tertiary sulci to map the "cognitive globe" of prefrontal cortex. J Cogn Neurosci 33:1698–1715.

Mufson EJ, Mesulam M-M (1982) Insula of the old world monkey. II: afferent cortical input and comments on the claustrum. J Comp Neurol 212:23–37.

Murphy AC, Bertolero MA, Papadopoulos L, Lydon-Staley DM, Bassett DS (2020) Multimodal network dynamics underpinning working memory. Nat Commun 11:3035.

Murray JD, Bernacchia A, Freedman DJ, Romo R, Wallis JD, Cai X, Padoa-Schioppa C, Pasternak T, Seo H, Lee D, Wang X-J (2014) A hierarchy of intrinsic timescales across primate cortex. Nat Neurosci 17:1661–1663.

Nee DE (2021) Integrative frontal-parietal dynamics supporting cognitive control. Elife 10:e57244.

Nee DE, D'Esposito M (2016) The hierarchical organization of the lateral prefrontal cortex. ELife 5:e12112.

Nee DE, Jahn A, Brown JW (2014) Prefrontal cortex organization: dissociating effects of temporal abstraction, relational abstraction, and integration with fMRI. Cereb Cortex 24:2377–2387.

Nee DE, D'Esposito M (2017) Causal evidence for lateral prefrontal cortex dynamics supporting cognitive control. Elife 6:e28040.

Picard N, Strick PL (1996) Motor areas of the medial wall: a review of their location and functional activation. Cereb Cortex 6:342–353.

Picard N, Strick PL (2001) Imaging the premotor areas. Curr Opin Neurobiol 11:663–672.

Pitts M, Nee DE (2022) Generalizing the control architecture of the lateral prefrontal cortex. Neurobiol Learn Mem 195:107688.

Power JD, Cohen AL, Nelson SM, Wig GS, Barnes KA, Church JA, Vogel AC, Laumann TO, Miezin FM, Schlaggar BL, Petersen SE (2011) Functional network organization of the human brain. Neuron 72:665–678.

Power JD, Barnes KA, Snyder AZ, Schlaggar BL, Petersen SE (2012) Spurious but systematic correlations in functional connectivity MRI networks arise from subject motion. Neuroimage 59:2142–2154.

Reynolds JR, O'Reilly RC, Cohen JD, Braver TS (2012) The function and organization of lateral prefrontal cortex: a test of competing hypotheses. PLoS One 7:e30284.

Sadaghiani S, D'Esposito M (2015) Functional characterization of the cingulo-opercular network in the maintenance of tonic alertness. Cereb Cortex 25:2763–2773.

Salehi M, Karbasi A, Barron DS, Scheinost D, Constable RT (2020) Individualized functional networks reconfigure with cognitive state. Neuroimage 206:116233.

Satterthwaite TD, Wolf DH, Erus G, Ruparel K, Elliott MA, Gennatas ED, Hopson R, Jackson C, Prabhakaran K, Bilker WB, Calkins ME, Loughead J, Smith A, Roalf DR, Hakonarson H, Verma R, Davatzikos C, Gur RC, Gur RE (2013) Functional maturation of the executive system during adolescence. J Neurosci 33:16249–16261.

Seeley WW (2019) The salience network: a neural system for perceiving and responding to homeostatic demands. J Neurosci 39:9878–9882.

Seeley WW, Menon V, Schatzberg AF, Keller J, Glover GH, Kenna H, Reiss AL, Greicius MD (2007) Dissociable intrinsic connectivity networks for salience processing and executive control. J Neurosci 27:2349–2356.

Shenhav A, Botvinick MM, Cohen JD (2013) The expected value of control: an integrative theory of anterior cingulate cortex function. Neuron 79:217–240.

Taren AA, Venkatraman V, Huettel SA (2011) A parallel functional topography between medial and lateral prefrontal cortex: evidence and implications for cognitive control. J Neurosci 31:5026–5031.

Theeuwes J (1993) Visual selective attention: a theoretical analysis. Acta Psychol (Amst) 83:93–154.

Uddin LQ (2015) Salience processing and insular cortical function and dysfunction. Nat Rev Neurosci 16:55–61.

Venkatraman V, Rosati AG, Taren AA, Huettel SA (2009) Resolving response, decision, and strategic control: evidence for a functional topography in dorsomedial prefrontal cortex. J Neurosci 29:13158–13164.

Vuorre M, Bolger N (2018) Within-subject mediation analysis for experimental data in cognitive psychology and neuroscience. Behav Res Methods 50:2125–2143.

Wang X, Wu Q, Egan L, Gu X, Liu P, Gu H, Yang Y, Luo J, Wu Y, Gao Z, Fan J (2019) Anterior insular cortex plays a critical role in interoceptive attention. Elife 8:e42265.

Yeo BT, Krienen FM, Sepulcre J, Sabuncu MR, Lashkari D, Hollinshead M, Roffman JL, Smoller JW, Zöllei L, Polimeni JR, Fischl B, Liu H, Buckner RL (2011) The organization of the human cerebral cortex estimated by intrinsic functional connectivity. J Neurophysiol 106:1125–1165.